

1 (Revised MS: es-2007-03245d)

2 **Determining optimal operation parameters for reducing PCDD/F emissions (I-TEQ**  
3 **values) from the iron ore sintering process by using the Taguchi experimental**  
4 **design**

5 *Yu-Cheng Chen<sup>1</sup>, Perng-Jy Tsai<sup>1,2</sup>, Jin-Luh Mou<sup>3</sup>*

6  
7 <sup>1</sup>Department of Environmental and Occupational Health, Medical College, National Cheng Kung  
8 University, 138, Sheng-Li Road, Tainan 70428, Taiwan;

9 <sup>2</sup>Sustainable Environment Research Center, National Cheng Kung University, 1 University Road,  
10 Tainan 70101, Taiwan;

11 <sup>3</sup>Department of Occupational Safety and Health, Chung Hwa University of Medical Technology, 89,  
12 Wenhwa 1st St., Rende Shiang, Tainan 71703, Taiwan

13  
14  
15 **\*Correspondence author:** Perng-Jy Tsai, Department of Environmental and Occupational Health,  
16 Medical College, National Cheng Kung University. 138, Sheng-Li Rd., Tainan 70428, Taiwan. Tel.:  
17 +886-6-2353535 ext. 5806; Fax: +886-6-2752484; E-mail address: [pjtsai@mail.ncku.edu.tw](mailto:pjtsai@mail.ncku.edu.tw)

## 18 Abstract

19 This study is the first one using the Taguchi experimental design to identify the optimal operating  
20 condition for reducing polychlorinated dibenzo-*p*-dioxins and dibenzofurans (PCDD/Fs) formations  
21 during the iron ore sintering process. Four operating parameters, including the water content (Wc; range  
22 = 6.0–7.0 wt %), suction pressure (Ps; range = 1000–1400 mmH<sub>2</sub>O), bed height (Hb; range = 500–600  
23 mm) and type of hearth layer (including sinter, hematite, and limonite), were selected for conducting  
24 experiments in a pilot scale sinter pot to simulate various sintering operating conditions of a real scale  
25 sinter plant. We found that the resultant optimal combination (Wc=6.5 wt%, Hb=500 mm, Ps=1000  
26 mmH<sub>2</sub>O, and hearth layer= hematite) could decrease the emission factor of total PCDD/Fs (total  
27 EF<sub>PCDD/Fs</sub>) up to 62.8% by reference to the current operating condition of the real-scale sinter plant  
28 (Wc=6.5 wt %, Hb = 550 mm, Ps = 1200 mmH<sub>2</sub>O, and hearth layer = sinter). Through the ANOVA  
29 analysis, we found that Wc was the most significant parameter in determining total EF<sub>PCDD/Fs</sub>  
30 (accounting for 74.7% of the total contribution of the four selected parameters). The resultant optimal  
31 combination could also enhance slightly in both sinter productivity and sinter strength (30.3 t/m<sup>2</sup>/day  
32 and 72.4%, respectively) by reference to those obtained from the reference operating condition (29.9  
33 t/m<sup>2</sup>/day and 72.2%, respectively). The above results further ensure the applicability of the obtained  
34 optimal combination for the real-scale sinter production without interfering its sinter productivity and  
35 sinter strength.

36 **Keywords:** PCDD/F formation, iron ore sintering, Taguchi experimental design, optimization,  
37 operation parameter

|    |  |
|----|--|
| 38 | <b>Running Title:</b> Optimizing operating parameters for reducing PCDD/F emissions by using the Taguchi |
| 39 | experimental design  |
| 40 | <b>Outline of Section Headers</b>  |
| 41 | Introduction   |
| 42 | Material and Methods   |
| 43 | Results and Discussion   |
| 44 | Literature cited   |

## 45 **Introduction**

46 Iron ore sintering is an agglomeration process to convert iron ore fines (raw mixture) into lumpy  
47 agglomerates. In the preliminary stage of sinter making process, water was sprayed onto the raw  
48 mixtures in the mixing drum to increase the granular sizes for enhancing the permeability of the sinter  
49 bed. During sintering, the raw mixtures were first ignited by gas-fueled (nature gas) burns situated at  
50 the beginning of the steel belt conveyer. Then, the sinter bed was heated to temperature ~1000 °C or  
51 above. Suction air passes through the sinter layer by means of wind legs and a fan, which moves the  
52 melting/combustion zone to the down layer to produce sintered products.

53 Mechanisms associated with the formations of dibenzo-*p*-dioxins and dibenzofurans (PCDD/Fs) in  
54 the sintering process are very complicated. Possible formation mechanisms might be related to  
55 precursor reactions (1-2) and combustion conditions of sinter raw mixtures (3-5). Particularly,  
56 PCDD/Fs could also be formed through de novo synthesis reaction in the dry zone of the sinter bed  
57 under various combustion conditions (2, 6). Many studies have indicated that the four operating  
58 parameters, including the water content (Wc) (7), suction pressure (Ps) (8), bed height (Hb) (9) and  
59 type of the hearth layer (10), are major factors affecting combustion conditions during the iron ore  
60 sintering process. Among these four parameters, the content of Wc in the sinter zone might affect the  
61 adsorption of PCDD/Fs on the surface of particles and the solubility of PCDD/Fs in water (7); the  
62 magnitude of Ps affects the air (or oxygen) supply which might play an important role in the oxygen-  
63 chlorine interactions related to PCDD/Fs formation (8); Hb affect the thickness and temperature profile  
64 of the combustion zone of the sinter bed and in consequence affects the contents of unburned  
65 hydrocarbon compounds during the sintering process (9); and the type of the hearth layer might affect  
66 the catalytic oxidation reaction associated with PCDD/F formations (10). All these operating parameters  
67 have been used to control the structure of the sinter bed to simulate various operation conditions for the  
68 sintering process in many studies (11-14).

69 Since the discovery of PCDD/Fs from the fly ash of a municipal solid waste incinerator (MSWI)  
70 (15), PCDD/F emissions from various emission sources, such as MSWI, power generation,

71 metallurgical process and chemical-industrial sources has become a significant environmental issue (16).  
72 Among them, PCDD/F emissions from iron ore sinter plants have been recognized as the most  
73 important source in many countries (17-19). To date, most sinter plants have installed various air  
74 pollution control devices (APCDs) for the control of PCDD/F emissions. Nevertheless, most sinter  
75 plants have faced the dilemma regarding how to continuously upgrade their APCDs in order to comply  
76 with stricter and stricter emission standards adopted in their countries. In order to comply with future  
77 PCDD/F emission standard and decrease the cost resulting from upgrading the end-pipe PCDD/F  
78 control devices, it is important to develop an effective method for directly reducing PCDD/F  
79 generations during the sintering process. It is known that the change of the contents of sinter raw  
80 mixture for reducing PCDD/F emissions would be impractical in the real situation. Therefore, to  
81 optimize operating conditions in order to reduce PCDD/F formations via de novo synthesis reaction in  
82 the dry zone of the sinter bed might provide a promising solution.

83 In principle, experimental design methods can be used to determine the optimal operating condition  
84 for a given purpose. For many years, experimental design methods originally developed by Fisher have  
85 been widely used in many industries (20). However, the use of the above methods might be subjected to  
86 their complexities and their requirement for a large number of experiments to be carried out as the  
87 number of the designed parameters increased. To solve the above problems, the Taguchi experimental  
88 design is considered as a less complicated method requiring only much smaller number of experiments  
89 to be conducted for identifying an optimal operation condition. The Taguchi experiment design is a  
90 powerful tool that provides a simple, efficient and systematic approach to optimize operating conditions  
91 under designated ranges of all selected parameters. The method is valuable when the designed  
92 parameters are qualitative and discrete. The method can used to optimize the performance  
93 characteristics through the settings of designed parameters and reduce the sensitivity of the system  
94 performance to sources of variation. In recent years, the Taguchi experiment design has been used in  
95 many industries to optimize the operating conditions for the waste water treatment and air pollution  
96 control (21-24). Therefore, in the current study the Taguchi experimental design is used to determine

97 the optimal operating combination for reducing PCDD/F formations during the sintering process. In  
98 addition, two important indexes (i.e., the sinter productivity and sinter strength) widely used for  
99 characterizing the quality of the sintering products were also examined to further ensure the optimal  
100 combination obtained from the Taguchi experiment design can be used in the real scale sinter plant.

101

## 102 **Material and Methods**

103 **The Pilot Scale Sinter Pot and Its Operating Procedures.** A pilot scale sinter pot was used in this  
104 study to simulate the real-scale sintering process (Fig. 1). This sinter pot included a pot body (inner  
105 diameter = 330 mm, height = 600 mm), an ignition hood, and a windbox connected to an exhaust duct.  
106 Six kilogram of hearth layer (particle diameters = 10–15 mm, thickness = 40 mm) were placed inside  
107 the sinter pot. During sintering, the designated ignition temperature in ignition hood was specified at  
108 1150–1200 °C for 1.5 minutes and then hold in another 1.5 minutes for keeping heat. During this period  
109 (i.e., starting from the ignition to the removal of the ignition hood) the suction pressure inside the sinter  
110 pot was controlled at 800 mmH<sub>2</sub>O by using an electromagnetic valve. After this, the suction pressure  
111 was raised to 1200 mmH<sub>2</sub>O and then kept constant throughout the end of the sintering process. The total  
112 sintering time was around 35 minutes depending on the experimental conditions.

113 The sintering raw mixture used in this study was directly obtained from the real-scale sinter plant. It  
114 consisted of the iron ore (52.8 wt %), coke breeze (4.0 wt %), anthracite (1.84 wt %), serpentine (0.42  
115 wt %), marble (1.98 wt %), slurry (0.56 wt %), and return fine (31.5 wt %; including return fine  
116 obtained from sinter plant and blast furnace), and mini-pellet (1.50 wt %) with mean granular sizes  
117 ranging from 1.0 to 6.3 mm. The sintering raw mixture was found with 5.81% FeO, 9.38% CaO, 1.44%  
118 MgO, 1.66% Al<sub>2</sub>O<sub>3</sub>, 4.79% SiO<sub>2</sub>, and total-Fe accounting for 57.5% total weight..

119 **Taguchi Experimental Design.** The working steps for the Taguchi experimental design include: (1)  
120 selection of operation parameters; (2) determination of the number of levels for each selected parameter;  
121 (3) selection of the appropriate orthogonal array and arrangement of operation parameters to the  
122 orthogonal array; (4) conducting experiments based on the arrangement of the orthogonal array; (5)

123 analysis of the experimental results using the S/N ratio and ANOVA analyses; (6) selection of the  
124 optimal combination of levels for the selected operation parameter; and (7) verification of the above  
125 optimal combination by conducting a confirmation experiment (25,26).

126 **Selected Operation Parameters, levels and Orthogonal Array.** Four operation parameters (and  
127 their testing ranges), including water content (Wc; 6.0–7.0 wt %), suction pressure (Ps; 1000–1400 mm  
128 H<sub>2</sub>O), bed height (Hb; 500–600 mm), and types of hearth layer (including sinter (containing 70% Fe<sub>2</sub>O<sub>3</sub>  
129 and 7% Fe<sub>3</sub>O<sub>4</sub>; Fe in total accounting for 58.1% of total weight), hematite (containing 88% Fe<sub>2</sub>O<sub>3</sub> and  
130 7% FeO·OH; Fe in total accounting for 64.1% of total weight), and limonite (containing 40% Fe<sub>2</sub>O<sub>3</sub>,  
131 45% FeO·OH and 6% H<sub>2</sub>O; Fe in total accounting for 63.3% of total weight)) were selected in this  
132 study. The selected ranges of the above four parameters were determined based on the past operation  
133 experience of the selected sinter plant and the published references (11, 27-28). A specific combination  
134 of the four selected operation parameters (i.e., Wc = 6.5 wt %, Ps = 1200 mmH<sub>2</sub>O, Hb = 550 mm, and  
135 type of hearth layer = sinter) being currently used in the real-scale sinter plant was served as the  
136 reference combination. Table 1 shows the selected three levels for each operation parameter based on its  
137 designated range. An  $L9(3^4)$  orthogonal array (with four columns and nine rows) was used in this study  
138 according to the Taguchi experimental design (Table 2) (25). Since the experimental design was  
139 orthogonal, it was possible to discriminate the effect of each individual parameter at each designated  
140 level. As shown in Table 2, nine combinations of the four selected operation parameters were chosen  
141 for conducting experiments. Subjected to the cost associated with PCDD/Fs samplings and sample  
142 analyses, each experiment were repeated twice (n=2) in this study.

143 **PCDD/Fs sampling.** For each experiment, the flue gas samples were collected from the duct located  
144 at the downstream of the windbox of the pilot sinter pot (see Fig 1) by using a Graseby Anderson stack  
145 isokinetic sampling system (compliance with US EPA Method 23). The sampling location was in  
146 accordance with the stack sampling criteria (i.e., in 8 times distance of duct diameter (8D) away from  
147 downstream of the curvature) and in 2 times distance of duct diameter (2D) away from upstream of the  
148 curvature) for preventing uncertainty caused by flow turbulence. Because the instability of the airstream

149 occurred during the first five minutes of the sintering process (i.e., the time needed for adjusting the  
150 suction pressure to reach the designated level), the flue gas of the first five minute was not collected. As  
151 a result, the sampling time for each flue gas sample was ~30 minutes.

152 **PCDD/Fs analysis.** Analysis of PCDD/Fs for all collected samples followed the US EPA modified  
153 Method 23 by an accredited lab in the Super Micro Mass Research and Technology Center of the  
154 Cheng-Shiu University. Each collected sample was first spiked with a known amount of the internal  
155 standard. Seventeen PCDD/F congeners in gas- and particle- phase were analyzed, respectively. For  
156 each collected sample, it was first extracted for 24 h, then the extract was concentrated, treated with  
157 concentrated sulfuric acid, and then followed by a series of sample cleanup and fractionation procedures.  
158 The eluate was concentrated to 1 mL, then transferred to a vial, and then further concentrated to nearly  
159 dryness by using a nitrogen stream. PCDD/Fs were analyzed by a high-resolution gas chromatography  
160 (HP 6970) / high-resolution mass spectrometry (HRGC/HRMS) with a DB-5 capillary column (60 m ×  
161 0.25 mm i.d., 0.25  $\mu$  m film thickness; J&W Scientific, CA, USA). Injections were made in splitless  
162 mode with a column oven temperature program of 150 °C, 30 °C/min to 220 °C (5 min), 1.5 °C/min to  
163 240 °C (5 min), than 15 °C /min to 310 °C (20 min). Injector and detector temperature were 250 °C and  
164 310 °C, respectively. Helium was used as carrier gas (1.2 mL/min). The HRMS (Micromass Autospec  
165 Ultimate) was equipped with a positive electron impact (EI+) source as 35ev electron energy and  
166 ionization temperature at 250 °C. The analyzer mode of the selected ion monitoring (SIM) was used  
167 with resolving power at 10,000.

168 Analysis of the serial dilution of PCDD/F standards showed that the method detection limits (MDL)  
169 of HRGC/HRMS was 0.127-2.27 pg. PCDD/F recovery efficiencies were determined by processing a  
170 solution containing with known PCDD/F concentrations through the same experimental procedure used  
171 for the samples. The recovery efficiency of PCDD/Fs varied between 74.3 % and 96.1 % and averaged  
172 84.8% in this study. The mean relative standard deviation (RSD) (%) of recovery efficiencies was  
173 18.6% (range 15.1–22.8%). The blank tests for PCDD/Fs were accomplished by the same procedure as



174 the recovery-efficiency tests without adding the known standard solution before extraction. Analysis of  
175 blanks showed no significant contamination.

176 Concentrations of PCDDs, PCDFs, gas- and particle-phase PCDD/Fs, and total PCDD/Fs of flue gas  
177 samples obtained from the nine selected experimental combinations were calculated. Because the  
178 purpose of the present study was aimed at reducing the environmental impact arising from PCDD/F  
179 emissions, therefore the I-TEQ concentration (i.e., ng I-TEQ/Nm<sup>3</sup>) was used to characterize the above  
180 concentrations. Considering the variations in flow rate, sintering time, and charging weight of feedstock  
181 among different experimental combinations, the emission factor of PCDD/Fs (EF<sub>PCDD/Fs</sub>; ng I-TEQ/kg-  
182 feedstock) were calculated for comparisons.

183 **Evaluation of sinter productivity and sinter strength.** The sinter productivity, expressed in tons  
184 per square meter of grate area of sintering machine per day, was calculated from the sintering time, the  
185 cross-sectional area of the pot grate, and the weight of sinter product recovered from the test (by  
186 removing the loss of the weight of hearth layer). The sinter strength was measured by using a modified  
187 ISO 3271 test method (29).

188 **Data analysis.** The S/N ratio based on the concept of the-lower-the-better was used to characterize  
189 EF<sub>PCDD/Fs</sub>. The S/N ratio ( $\eta$ ) was defined as (25):

190 
$$\eta = -10 \log (\text{M.S.D.}) \quad (1)$$

191 Where, mean-square deviation (M.S.D.) was the calculated variance for the characteristic value  $y$ .  
192 The S/N ratio in decibel (dB) units was used due to the value of ten times the common log of equation  
193 (Eqs. 1) for comparison. The M.S.D. characterized the-lower-the-better was obtained as:

194 
$$\text{M.S.D.} = \frac{1}{n} \sum_{i=1}^n y_i^2 \quad (2)$$

195 Where,  $n$  was number of test, and  $y_i$  was the value of EF<sub>PCDD/Fs</sub> obtained from the  $i$ th test. The  
196 predicted S/N ratio (or EF<sub>PCDD/Fs</sub>) ( $\beta$ ) for the optimal combination could be calculated as:

197 
$$\beta = \eta_m + \sum_{i=1}^o (\bar{\eta}_i - \eta_m) \quad (3)$$

198 Where,  $\eta_m$  was the total mean S/N ratio,  $\bar{\eta}_i$  was the maximum S/N ratio (or the minimum  $EF_{PCDD/Fs}$ )  
199 obtained from the  $i$ th parameters in their three designated levels, and  $o$  was the number of our selected  
200 parameters.

201 In addition, the analysis of variance (ANOVA) was used to investigate the effect of each individual  
202 parameter on  $EF_{PCDD/Fs}$ .

203

## 204 **Results and Discussion**

205 **Concentrations and characteristics of PCDD/Fs emitted from the sinter process.** Table 3 shows  
206 concentrations of PCDDs, PCDFs, gas- and particle-phase PCDD/Fs, and total PCDD/Fs of flue gas  
207 samples obtained from the nine selected experimental combinations. The mean total PCDD/F  
208 concentration was 0.940 ng I-TEQ/Nm<sup>3</sup> (range = 0.279–1.70 ng I-TEQ/Nm<sup>3</sup>), which was mostly  
209 contributed by gas-phase PCDD/Fs (in average accounting for 63% of total PCDD/Fs). These levels  
210 were similar to those reported by Wang et al. (30), and Anderson and Fisher (18). PCDFs had a higher  
211 fraction (53.5–83.8 %) in total PCDD/Fs in all experimental combinations than that of PCDDs  
212 (16.2–46.5 %). Considering intrinsic differences in flow rate, sintering time and charging weight among  
213 the nine selected experimental combinations, Table 3 also shows the total PCDD/F emission factor  
214 (total  $EF_{PCDD/Fs}$ ) for each combination. We found that the mean total  $EF_{PCDD/Fs}$  for the nine selected  
215 experimental combinations was 5.16 ng I-TEQ/kg-feedstock (range = 1.01–9.37 ng I-TEQ/kg-  
216 feedstock). However, it should be noted that the trend in magnitude of total  $EF_{PCDD/Fs}$  was somewhat  
217 different from that of total PCDD/F concentrations for the nine selected experimental combinations.  
218 The above result clearly indicates the importance of using total  $EF_{PCDD/Fs}$  to determine the optimal  
219 combination for reducing PCDD/F emissions from the sintering process.

220 Figure 2 showed the congener profiles of the 2,3,7,8-substituted PCDD/Fs (mean and range) of the  
221 nine selected experimental combinations. The most abundant congeners collected from the sinter pot,

222 presented in sequence, were 2,3,7,8-TeCDF, 2,3,4,7,8-PeCDF, 1,2,3,4,6,7,8-HxCDF, 1,2,3,7,8-PeCDF,  
223 and OCDD. The above results were similar to those presented in other studies (18, 30).

224 **S/N ratios and ANOVA analysis.** In this study, the total  $EF_{PCDD/Fs}$  obtained from the nine selected  
225 experimental combinations were used to calculate S/N ratio. The S/N ratios of the four selected  
226 parameters in three designated levels according to the orthogonal array experimental arrangement were  
227 presented in Table 4. We found that the resultant S/N ratios fell to the range from -0.69 to -19.6 dB.  
228 Table 5 shows mean S/N ratios of the four selected parameters in each of their three designated levels.  
229 For each selected parameter, the difference between maximum S/N ratio and its corresponding  
230 minimum S/N ratio (i.e., max-min) represents the effect of the given parameter on determining total  
231  $EF_{PCDD/Fs}$ . Based on this, we found that the effects in sequence for the four selected parameters on total  
232  $EF_{PCDD/Fs}$  were: Wc (12.3 dB), Ps (4.15 dB), hearth layer (3.45 dB) and Hb (3.15 dB). Figure 3 shows  
233 the trend of the resultant S/N ratios for each selected parameters at the three designated levels affecting  
234 total  $EF_{PCDD/Fs}$ . Both Ps and Hb shared the same trend in their resultant S/N ratios (i.e., first decreased  
235 then increased). The above trend was different from that of Wc (i.e., first increased then decreased) and  
236 hearth layer. The combination of Wc (=6.50 wt %), Ps (=1000 mmHg), Hb (=500 mm), and hearth  
237 layer (=hematite) were found with the highest S/N ratio for each of the four selected parameters, and  
238 hence was considered as the optimal operation condition for reducing PCDD/F emissions.

239 In this study, the ANOVA analysis was used to prioritize to effects of the four selected parameters on  
240 determining total  $EF_{PCDD/Fs}$ . Result shows that Wc ( $p < 0.01$ ) was the most significant parameter  
241 accounting for 74.7% of the total contribution of the four selected parameters (Table 6). The above  
242 result was consistent with that found in Suzuki et al. (4) and Li et al. (31). Here, it should be noted that  
243 the optimal Wc was found at the middle level (i.e., 6.5 wt %) might be worth further discussion. Kasai  
244 et al. (32) and Haga et al. (33) have indicated that the increase of Wc in sinter raw mixtures could  
245 increase the permeability of sintering bed and combustion efficiency (due to the abundant coke breezes  
246 and limestone fines coating on the surface of particles), and hence results in reducing PCDD/F  
247 formation during sintering processes. On the other hand, two other studies have indicated that the

248 increase of Wc might lead to the increase of PCDD/F emissions because the adsorption of PCDD/Fs on  
249 the surface area of sinter raw mixtures was partly replaced by the water molecules (4, 31). Based on  
250 these, it is not so surprising to see that the lowest total  $EF_{PCDD/Fs}$  was found at the middle level (i.e., 6.5  
251 wt %) rather than at 6.0 wt % or 7.0 wt %. The optimal Ps and Hb were found at their corresponding  
252 lowest levels (1000 mmH<sub>2</sub>O and 500 mm, respectively). The above results might be because the lower Ps  
253 and Hb might result in a wider combustion/melting zone in the sinter bed, leading to a more complete  
254 coke combustion and less PCDD/F formation during the sintering process. For the type of hearth layer,  
255 we found that the use of hematite could slightly decrease total  $EF_{PCDD/Fs}$  in comparison with the use of  
256 sinter as the hearth layer of the sinter pot, although the above effect was not significant ( $p=0.187$ ).  
257 Studies have reported that Fe<sub>2</sub>O<sub>3</sub> did play an important role in catalytic oxidation of carbon monoxide  
258 and polyethylene (34-35). The higher Fe<sub>2</sub>O<sub>3</sub> content might result in the less PCDD/F formation. The  
259 above inference is consistent with what we found in the three selected types of hearth layer in their  
260 Fe<sub>2</sub>O<sub>3</sub> contents (i.e., hematite (88%) > sinter (70%) > limonite (40%)). The insignificant effect  
261 associated with the types of hearth layer used in this study deserves further discussion. It might mainly  
262 be because the depth of the hearth layer was too thin to have sufficient reaction time for the formation of  
263 PCDD/Fs during sintering process. However, it should be noted that other physical parameters of hearth  
264 layer, such as the particle size and porosity, could also be important factors affecting PCDD/F  
265 formations. Considering the combined effect of all these physical factors on PCDD/F formations were  
266 too complicated, which warrants the need for further research in the future.

#### 267 **Comparison PCDD/F emissions between the reference and the optimal operation combination.**

268 Table 7 shows total  $EF_{PCDD/Fs}$  and S/N ratios obtained from the reference combination (i.e., Wc=6.5 wt  
269 %, Ps=1200 mmH<sub>2</sub>O, Hb=550 mm, and hearth layer = sinter) and the resultant optimal combination  
270 (i.e., Wc=6.50 wt %, Ps=1000 mmHg, Hb=500 mm, and hearth layer=hematite). The total  $EF_{PCDD/Fs}$  and  
271 its corresponding S/N ratio for the reference combination were found as 3.09 ng I-TEQ/kg-feedstock  
272 and -10.8 dB, respectively. For the optimal combination, its total  $EF_{PCDD/Fs}$  and S/N ratio (predicted  
273 based on Eqs. 3) were found as 1.01 ng I-TEQ/kg-feedstock and -0.694 dB, respectively. The difference

274 in the above two S/N ratios (= 10.1 dB) indicating that the use of the optimal combination would result  
275 in a decrease in total  $EF_{PCDD/Fs}$  up to 67.3% in comparison with the reference combination. For  
276 confirmation purpose, experiments were conducted based on the specification of the resultant optimal  
277 combination. The resultant total  $EF_{PCDD/Fs}$  and its corresponding S/N ratio were found as 1.15 ng I-TEQ/  
278 kg-feedstock and -1.21 dB, respectively. The increase in S/N ratio from the reference combination to  
279 the optimal combination (confirmation experiment) was 9.59 dB, and the resultant decrease in total  
280  $EF_{PCDD/Fs}$  was up to 62.8%. The above results further confirm the applicability of the obtained optimal  
281 combination for reducing PCDD/F formations during the sintering process.

### 282 **Sinter productivity and sinter strength of the reference and optimal operation combination.**

283 Although the resultant optimal combination was able to reduce PCDD/F emissions, it is important to  
284 examine its impact on the sinter productivity and sinter strength for practical reason. In this study, we  
285 found that the sinter productivity and sinter strength for the reference combination were 29.9 t/m<sup>2</sup>/day  
286 and 72.2%, respectively. The above values were slightly lower than that of the optimal combination  
287 (30.3 t/m<sup>2</sup>/day and 72.4%, respectively). Therefore, it is concluded that the use of the optimal  
288 combination for the sintering process could effectively reduce PCDD/F emissions without interfering  
289 with both the quality and quantity of its sinter products.

### 290 **Acknowledgements**

291 We would like to thank the China Steel Corporation (CSC) in Taiwan for funding and providing  
292 testing materials and facilities for this research project.

293 **Literature Cited**

- 294 (1). Milligan, M. S.; Altwicker, E. R. Chlorophenol Reactions on Fly Ash. 1. Adsorption/Desorption  
295 Equilibria and Conversion to Polychlorinated Dibenzo-p-dioxins. *Environ. Sci. Technol.* **1996**,  
296 *30*, 225-229.
- 297 (2). Kasai, E.; Hosotani, Y.; Kawaguchi, T.; Nushiro, K.; Aono, T. Effect of additives on the dioxins  
298 emissions in the iron ore sintering process. *ISIJ Int.* **2001**, *41*, 93-97.
- 299 (3). Harjanto, S.; Kasai, E.; Terui, T.; Nakamura, T. Behavior of dioxin during thermal remediation  
300 in the zone combustion process. *Chemosphere* **2002**, *47*, 687-693.
- 301 (4). Suzuki, K.; Kasai, E.; Aono, T.; Yamazaki, H.; Kawamoto, K. De novo formation  
302 characteristics of dioxins in the dry zone of an iron ore sintering bed. *Chemosphere* **2004**, *54*,  
303 97-104.
- 304 (5). Kasai, E.; Harjanto, S.; Terui, T.; Nakamura, T.; Waseda, Y. Thermal remediation of PCDD/Fs  
305 contaminated soil by zone combustion process. *Chemosphere* **2000**, *41*, 857-864.
- 306 (6). Buekens, A.; Stieglitz, L.; Hell, K.; Huang, H.; Segers, P. Dioxins from thermal and  
307 metallurgical processes: recent studies for the iron and steel industry. *Chemosphere* **2001**, *42*,  
308 729-735.
- 309 (7). Harjanto, S.; Kasai, E.; Terui, T.; Nakamura, T. Formation and transport of PCDD/Fs in the  
310 packed bed of soil containing organic chloride during a thermal remediation process.  
311 *Chemosphere* **2002**, *49*, 217-224.
- 312 (8). Tan, P.; Hurtado, I.; Neuschutz, D.; Eriksson, G. Thermodynamic Modeling of PCDD/Fs  
313 Formation in Thermal Processes. *Environ. Sci. Technol.* **2001**, *35*, 1867-1874.

- 314 (9). Mitterlehner, J.; Loeffler, G.; Winter, F.; Hofbauer, H.; Schmid, H.; Zwittag, E.; Buegler, T. H.;  
315 Pammer, O.; Stiasny, H. Modeling and simulation of heat front propagation in the iron ore  
316 sintering process. *ISIJ Int.* **2004**, *44*, 11-20.
- 317 (10). Cieplik, M. K.; Carbonell, J. P.; Munoz, C.; Baker, S.; Kruger, S.; Liljelind, P.; Marklund, S.;  
318 Louw, R. On Dioxin Formation in Iron Ore Sintering. *Environ. Sci. Technol.* **2003**, *37*, 3323-  
319 3331.
- 320 (11). Nath, N. K.; Mitra, K. Optimisation of suction pressure for iron ore sintering by genetic  
321 algorithm. *Ironmaking and Steelmaking* **2004**, *31*, 199-206.
- 322 (12). Maeda, T.; Fukumoto, C.; Matsumura, T.; Nishioka, K.; Shimizu, M. Effect of adding moisture  
323 and wettability on granulation of iron ore. *ISIJ Int.* **2005**, *45*, 477-484.
- 324 (13). Kawaguchi, T.; Kamijo, C.; Matsumura, M. The sintering behavior of raw material bed placing  
325 large particles. *Tetsu-to-Hagane* **2006**, *92*, 779-787.
- 326 (14). Yang, W.; Choi, S.; Choi, E. S.; Ri, D. W.; Kim, S. Combustion characteristics in an iron ore  
327 sintering bed—evaluation of fuel substitution. *Combustion and Flame* **2006**, *145*, 447-463.
- 328 (15). Olie, K.; Vermeulen, P. L.; Hutzinger, O. Chlorodibenzo-p-dioxins and chlorodibenzofurans are  
329 trace components of fly ash and flue gas of some municipal incinerators in The Netherlands.  
330 *Chemosphere* **1977**, *6*, 455-459.
- 331 (16). Oh, J. E.; Choi, S. D.; Lee, S. J.; Chang, Y. S. Influence of a municipal solid waste incinerator  
332 on ambient air and soil PCDD/Fs levels. *Chemosphere* **2006**, *64*, 579-587.
- 333 (17). Alcock, R. E.; Gemmill, R.; Jones, K. C. Improvements to the UK PCDD/F and PCB  
334 atmospheric emission inventory following an emissions measurement programme.  
335 *Chemosphere* **1999**, *38*, 759-770.

- 336 (18). Anderson, D. R.; Fisher, R. Sources of dioxins in the United Kingdom: the steel industry and  
337 other sources. *Chemosphere* **2002**, *46*, 371-381.
- 338 (19). Aries, E.; Anderson, D. R.; Fisher, R.; Fray, T. A. T.; Hemfrey, D. PCDD/F and "Dioxin-like"  
339 PCB emissions from iron ore sintering plants in the UK. *Chemosphere* **2006**, *65*, 1470-1480.
- 340 (20). Fisher, R. A. Statistical Methods for Research Workers, Oliver and Boyd, London, **1925**.
- 341 (21). Bendell, A.; Disney, J.; Pridmore, W. A. Taguchi Methods: Applications in World Industry, IFS  
342 Publications, UK, 1989.
- 343 (22). Raj, C. B. C.; Quen, H. L. Advanced oxidation processes for wastewater treatment: Optimization  
344 of UV/H<sub>2</sub>O<sub>2</sub> process through a statistical technique. *Chemical Engineering Science* **2005**, *60*,  
345 5305 – 5311
- 346 (23). Chyang, C. S.; Wu, K. T.; Lin, C. S. Emission of nitrogen oxides in a vortexing fluidized bed  
347 combustor. *Fuel* **2007**, *86*, 234–243.
- 348 (24). Yang, J.; Peng, J.; Guo, R.; Liu, K. C.; Jia, J. P.; Xu, D. L. Optimization and thermodynamic  
349 assessment of ferrite (Fe<sub>3</sub>O<sub>4</sub>) synthesis in simulated wastewater. *Journal of Hazardous*  
350 *Materials* **2007**, *149*, 106-114.
- 351 (25). Taguchi, G. Introduction to Quality Engineering, Asian Productivity Organization: Tokyo,  
352 Japan, **1987**; pp 121-132.
- 353 (26). Yang, W. H.; Tarng, Y. S. Design optimization of cutting parameters for turning operations  
354 based on the Taguchi method. *Journal of Materials Processing Technology* **1998**, *84*, 122-129.
- 355 (27). Yang, W.; Ryu, C.; Choi, S.; Choi, E.; Lee, D.; Huh, W. Modeling of combustion and heat  
356 transfer in an iron ore sintering bed with considerations of multiple solid phases. *ISIJ*  
357 *International* **2004**, *44*, 492-499.



- 358 (28). Oyama, N.; Sato, H.; Takeda, K.; Ariyama, T.; Masumoto, S.; Jinno, T.; Fujii, N. Development  
359 of coating granulation process at commercial sintering plant for improving productivity and  
360 reducibility. *ISIJ International* **2005**, *45*, 817-826.
- 361 (29). International Organization for Standardization (ISO) 3271, Iron ores – Determination of tumble  
362 strength. Third edition, **1995**.
- 363 (30). Wang, L. C.; Lee, W. J.; Tsai, P. J.; Lee, W. S.; Chang-Chien, G. P. Emissions of  
364 polychlorinated dibenzo-p-dioxins and dibenzofurans from stack flue gases of sinter plants.  
365 *Chemosphere* **2003**, *50*, 1123-1129.
- 366 (31). Li, X. D.; Zhang, J.; Yan, J. H.; Chen, T.; Lu, S. Y.; Cen, K. F. Effect of water on catalyzed de  
367 novo formation of polychlorinated dibenzo-p-dioxins and polychlorinated dibenzofurans.  
368 *Journal of Hazardous Materials* **2006**, *137*, 57-61.
- 369 (32). Kasai, E.; Rankin, W. J.; Gannon, J. F. The Effect of Raw Mixture Properties on Bed  
370 Permeability during Sintering. *ISIJ Int.* **1989**, *29*, 33-42.
- 371 (33). Haga, T.; Ohshio, A.; Nakamura, K.; Kozono, T. Control technique of the melting reaction in  
372 sintering process by the fine part selective granulation of clayish iron ores. *Tetsu-to-Hagane*  
373 **1997**, *83*, 103-108.
- 374 (34). Imai, T.; Matsui, T.; Fujii, Y.; Nakai, T.; Tanaka, S. Oxidation catalyst of iron oxide  
375 suppressing dioxin formation in polyethylene combustion. *J Mater Cycles Waste Manag* **2001**,  
376 *3*, 103–109.
- 377 (35). Hung, W. T.; Lin, C. F. Use of regenerated ferric oxide for CO destruction and suppressing  
378 dioxin formation in flue gas in a pilot-scale incinerator. *Chemosphere* **2003**, *53*, 727-735.

379

380 List of Figures

381 FIGURE 1. The schematic of the pilot scale sinter pot

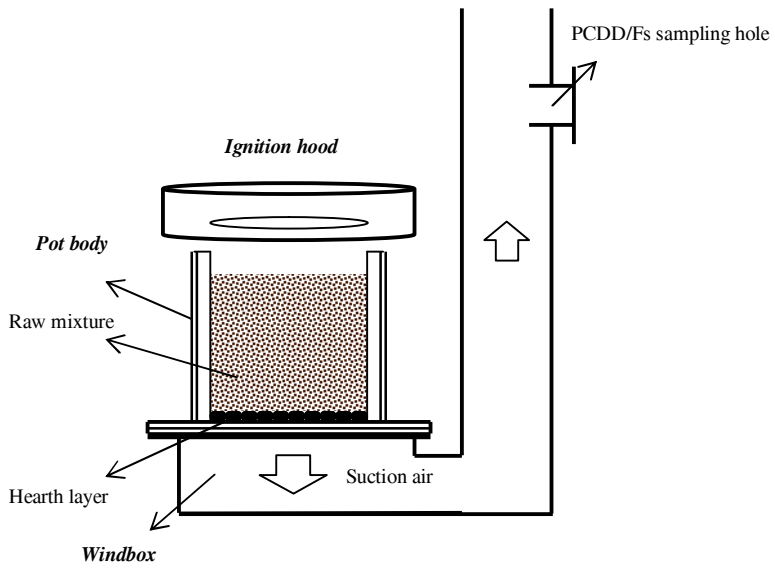
382 FIGURE 2. Congener profiles of seventeen PCDD/F congeners in the flue gases of sinter pot operated  
383 under the nine experimental combinations

384 FIGURE 3. Mean S/N ratios of the four selected operation parameters at the three designated levels

385

386

387



388

389 FIGURE 1. The schematic of the pilot scale sinter pot

390

391

392

393

394

395

396

397

398

399

400

401

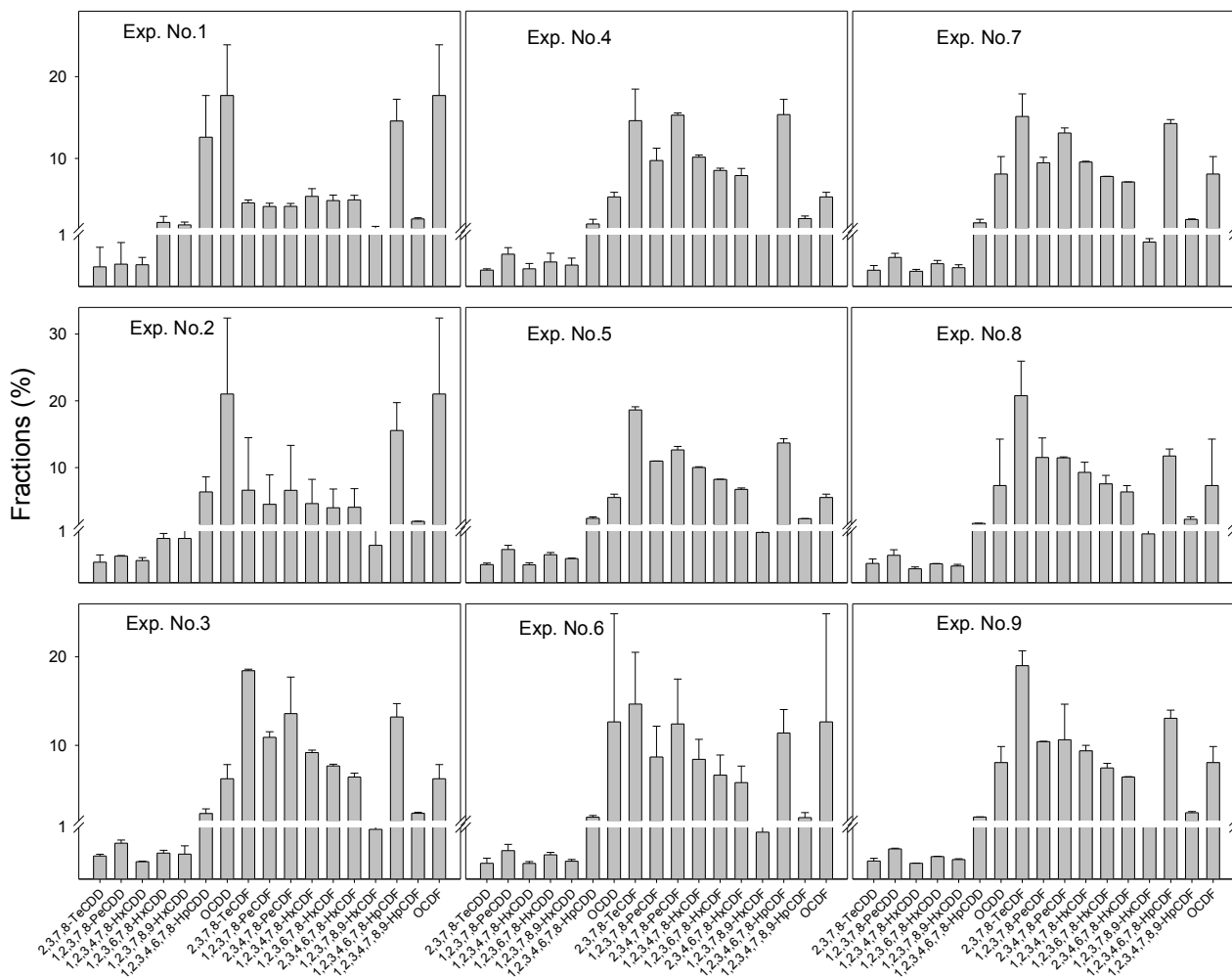
402

403

404

405

406



407 FIGURE 2. Congener profiles of seventeen PCDD/F congeners in the flue gases of sinter pot operated

408 under the nine experimental combinations

409

410

411

412

413

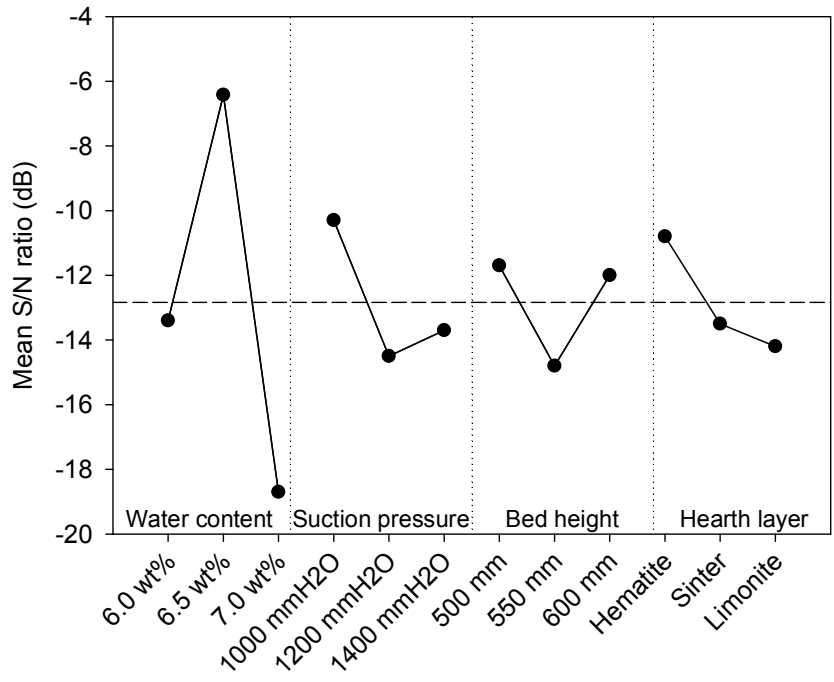
414

415

416

417

418



419

FIGURE 3. Mean S/N ratios of the four selected operation parameters at the three designated levels

420 **List of Tables**

421 TABLE 1. Operating parameters and their selected levels for the studied sintering process

422 TABLE 2. The nine designed experiment combinations of the four selected parameters for the Taguchi  
423  $L_9$  orthogonal array

424 TABLE 3. PCDDs, PCDFs, gas- and particle-phase PCDD/Fs, and total PCDD/Fs emission  
425 concentrations (ng I-TEQ/Nm<sup>3</sup>) in the flue gas of the nine designed experimental  
426 combinations and their corresponding emission factors of total PCDD/Fs (EF<sub>PCDD/Fs</sub>; ng I-  
427 TEQ/kg-feedstock)

428 TABLE 4. The resultant S/N ratios for the nine experiment combinations of the Taguchi  $L_9$  orthogonal  
429 array

430 TABLE 5. Mean S/N ratios for the four selected operation parameters in three designated levels

431 TABLE 6. Results of the analysis of variance for the four selected parameters

432 TABLE 7. The emitted total EF<sub>PCDD/Fs</sub> and its corresponding S/N ratio obtained from the reference  
433 operation combination and optimal operation combination (including both predicted and  
434 that obtained from the confirmation experiments)

435

**Table 1.** Operating parameters and their selected levels for the studied sintering process

| Operation parameter   | Unit               | Level 1 <sup>a</sup> | Level 2  | Level 3  |
|-----------------------|--------------------|----------------------|----------|----------|
| Water content (Wc)    | wt %               | 6.5                  | 6.0      | 7.0      |
| Suction pressure (Ps) | mmH <sub>2</sub> O | 1200                 | 1000     | 1400     |
| Bed Height (Hb)       | mm                 | 550                  | 500      | 600      |
| Hearth layer          | -                  | Sinter               | Hematite | Limonite |

<sup>a</sup>: Reference combination

**Table 2.** The nine designed experiment combinations of the four selected parameters for the Taguchi  $L_9$  orthogonal array

| Experiment combination | Water content | Suction pressure | Bed Height | Hearth layer |
|------------------------|---------------|------------------|------------|--------------|
| 1                      | 1             | 1                | 1          | 1            |
| 2                      | 1             | 2                | 2          | 2            |
| 3                      | 1             | 3                | 3          | 3            |
| 4                      | 2             | 1                | 2          | 3            |
| 5                      | 2             | 2                | 3          | 1            |
| 6                      | 2             | 3                | 1          | 2            |
| 7                      | 3             | 1                | 3          | 2            |
| 8                      | 3             | 2                | 1          | 3            |
| 9                      | 3             | 3                | 2          | 1            |

**Table 3.** PCDDs, PCDFs, gas- and particle-phase PCDD/Fs, and total PCDD/Fs emission concentrations (ng I-TEQ/Nm<sup>3</sup>) in the flue gas of the nine designed experimental combinations and their corresponding emission factors of total PCDD/Fs (EF<sub>PCDD/Fs</sub>; ng I-TEQ/kg-feedstock)

| Emission concentration      | Experimental combination |       |       |       |       |       |       |       |       |
|-----------------------------|--------------------------|-------|-------|-------|-------|-------|-------|-------|-------|
|                             | 1                        | 2     | 3     | 4     | 5     | 6     | 7     | 8     | 9     |
| PCDDs                       | 0.187                    | 0.040 | 0.043 | 0.059 | 0.049 | 0.079 | 0.055 | 0.075 | 0.119 |
| PCDFs                       | 0.719                    | 0.238 | 0.529 | 0.952 | 0.666 | 1.15  | 0.846 | 1.08  | 1.58  |
| Gas-phase PCDD/Fs           | 0.564                    | 0.196 | 0.365 | 0.518 | 0.325 | 0.752 | 0.570 | 0.963 | 1.21  |
| Particle-phase PCDD/Fs      | 0.342                    | 0.082 | 0.206 | 0.492 | 0.390 | 0.477 | 0.331 | 0.191 | 0.485 |
| Total PCDD/Fs               | 0.906                    | 0.279 | 0.571 | 1.01  | 0.715 | 1.23  | 0.901 | 1.15  | 1.70  |
| Emission factor             |                          |       |       |       |       |       |       |       |       |
| Total EF <sub>PCDD/Fs</sub> | 3.09                     | 1.01  | 2.44  | 5.80  | 3.45  | 5.05  | 7.40  | 9.37  | 8.79  |

438

439

440

441

442

443

444



**Table 4.** The resultant S/N ratios for the nine experiment combinations of the Taguchi  $L_9$  orthogonal array

| Experiment combination | Water content (%) | Suction pressure (mmH <sub>2</sub> O) | Bed height (mm) | Hearth layer | S/N ratio (dB) |
|------------------------|-------------------|---------------------------------------|-----------------|--------------|----------------|
| 1                      | 6.5               | 1200                                  | 550             | sinter       | -10.8          |
| 2                      | 6.5               | 1000                                  | 500             | hematite     | -0.69          |
| 3                      | 6.5               | 1400                                  | 600             | limonite     | -7.77          |
| 4                      | 6                 | 1200                                  | 500             | limonite     | -15.3          |
| 5                      | 6                 | 1000                                  | 600             | sinter       | -10.7          |
| 6                      | 6                 | 1400                                  | 550             | hematite     | -14.1          |
| 7                      | 7                 | 1200                                  | 600             | hematite     | -17.4          |
| 8                      | 7                 | 1000                                  | 550             | limonite     | -19.6          |
| 9                      | 7                 | 1400                                  | 500             | sinter       | -19.1          |

**Table 5.** Mean S/N ratios for the four selected operation parameters in three designated levels

| Operation parameter   | Mean S/N ratio (dB) |         |         |         | Rank |
|-----------------------|---------------------|---------|---------|---------|------|
|                       | Level 1             | Level 2 | Level 3 | Max–Min |      |
| Water content (Wc)    | -6.42               | -13.4   | -18.7   | 12.3    | 1    |
| Suction pressure (Ps) | -14.5               | -10.3   | -13.7   | 4.15    | 2    |
| Bed Height (Hb)       | -14.8               | -11.7   | -12.0   | 3.15    | 4    |
| Hearth layer          | -13.5               | -10.8   | -14.2   | 3.45    | 3    |

452

**Table 6.** Results of the analysis of variance for the four selected parameters

453

| Operation parameter   | DOF <sup>a</sup> | SS <sup>b</sup> | Var <sup>c</sup> | $F^d$ | $p$ -value | Contribution (%) |
|-----------------------|------------------|-----------------|------------------|-------|------------|------------------|
| Water content (Wc)    | 2                | 456             | 228              | 22.9  | <0.001     | 74.7             |
| Suction pressure (Ps) | 2                | 58.0            | 29.0             | 2.92  | 0.105      | 9.49             |
| Bed Height (Hb)       | 2                | 36.4            | 18.2             | 1.83  | 0.215      | 5.95             |
| Hearth layer          | 2                | 40.3            | 20.1             | 2.03  | 0.187      | 6.59             |
| Error                 | 9                | 89.4            | 9.93             | -     | -          | 3.25             |
| Total                 | 17               | 680             | 305              | -     | -          | 100              |

<sup>a</sup>Degree of freedom; <sup>b</sup>Sum of squares; <sup>c</sup>Mean square; <sup>d</sup> $F$ -test**Table 7.** The emitted total EF<sub>PCDD/Fs</sub> concentration and its corresponding S/N ratio obtained from the reference operation combination and optimal operation combination (including both predicted and that obtained from the confirmation experiments).

| Testing results  | Reference operation combination | Optimal operation combination |              |
|--|---------------------------------|-------------------------------|--------------|
|  |                                 | Prediction                    | Confirmation |
| Total EF <sub>PCDD/Fs</sub><br>( ng I-TEQ/kg-feedstock ) | 3.09                            | 1.01                          | 1.15         |
| S/N ratio (dB)   | -10.8                           | -0.694                        | -1.21        |